

The Design of Pressure Control System using PD Controller for Light Duty Electric Vehicle

Patiparn Intacharoen¹, Chaikut Sumpavakup², Kokiatt Aodsup³ and Soontorn Odngam^{2*}

¹ Department of Power Engineering Technology, College of Industrial Technology,
King Mongkut's University of Technology North Bangkok

² Research Centre for Combustion Technology and Alternative Energy – CTAE and
College of Industrial Technology, King Mongkut's University of Technology North Bangkok

³ Department of Electrical Engineering, Rajamangala University of Technology Lanna, Tak

* Corresponding author, E-mail: soontorn.o@cit.kmutnb.ac.th

Received: 7 November 2024; Revised: 20 December 2024; Accepted: 8 January 2025

Online Published: 22 April 2025

Abstract: This article describes a control method for braking oil pressure control based on a hydraulic brake control system for light-duty electric vehicles. This research aims to investigate and develop an automated braking system to lessen the possibility of accidents and also prevent frontal collisions of vehicles. In this study, a brake management system was designed with a PD controller and a linear motor actuator was chosen to control the brake oil pressure. System identification of the mathematical model is necessary to investigate the relationship between input and output responses in the linear model's range. In order to gain insight into the behavior of this system, a mathematical model was investigated and estimated, and the ideal values for the PD controller were determined as well. These estimated values were then utilized in an optimization process. Using the parameter estimation in the MATLAB Simulink, the control parameters, with the proportional gain value at 27.9606 and the derivative gain at 32.0490, were identified. The developed braking system implemented in a light-duty electric vehicle showed that it could effectively regulate the brake oil pressure using the prescribed parameter. The error value was not more than ± 8 psi of the specified value. These findings highlight the potential of the system's applicability to extend to large vehicles further.

Keywords: Brake system; DC motor; System identification; PD controller

1. Introduction

Currently, the automotive industry plays a crucial and influential role in shaping human daily life due to the necessity of transportation for various commercial and daily activities. The increasing number of registered vehicles in Thailand from 2018 to 2021, as the Department of Land Transport reported, reflects a growth rate of 1.91% per year, reaching approximately one million vehicles annually. With the growing number of vehicles, there is a heightened awareness of the environmental and health impacts, leading to an increased interest in advanced and environmentally friendly technologies. Electric vehicles (EVs) have witnessed a significant surge in popularity compared to other vehicle types, driven by continuous advancements in contemporary and cutting-edge technologies [1]. The current focus on developing automated driving systems in modern vehicles aims to enhance user convenience and safety [2]. Safety systems have gained widespread popularity, especially considering the rising number of road accidents. According to accident data, there was an alarming increase in road fatalities in the first two quarters of 2023 compared to the previous year. One significant safety feature being developed and integrated into vehicles is the Automatic Emergency Braking (AEB) system [3].

Because cars play such an important function in daily life, the safety system is essential to reducing the number of people who die in land-based travel accidents. Given the high number of fatalities resulting from auto accidents, safety systems are essential for lowering incidences and boosting motorist trust. As a result, several automakers have invested a great deal of time and resources into creating safety features that reduce collisions and increase road user confidence [4-6].

The research presented above aims to contribute to the development of an AEB system, specifically for commercial electric vehicles with limited operational space. This research considers controlling the brake fluid pressure using a PD controller [7-9] by estimating and optimizing various direct current (DC) motor parameters. This involves approximating and optimizing the motor parameters to determine suitable control values. These control values will then be applied to regulate the hydraulic brake pressure at 200 psi. The experimental results will be used to analyze the system's performance and assess the effectiveness of this control strategy.

2. Brake System Design

A brake system design is a critical aspect in the automotive engineering domain, encompassing various components and technologies to ensure optimal vehicle safety and performance. The brake

system is fundamental for controlling and decelerating the vehicle, contributing significantly to overall road safety. Several factors influence the design of an effective brake system, including the vehicle's weight, speed, intended use, and environmental conditions. Engineers employ advanced technologies and materials to enhance braking efficiency, reduce stopping distances, and ensure consistent performance under varying circumstances.

The design of a brake system involves a comprehensive consideration of mechanical, hydraulic, and electronic components tailored to meet safety standards, vehicle specifications, and technological advancements. The continuous evolution of brake system design reflects the automotive industry's commitment to enhancing both vehicle performance and road safety.

From Fig. 1, in consideration of designing a brake system for a vehicle while the vehicle is in motion at any given speed, the braking action introduces a delay. This delay can be analyzed by categorizing the evaluation into three parts. Part 1 examines front-wheel braking, Part 2 addresses rear-wheel braking, and Part 3 investigates four-wheel braking.

Considering the braking force at the rear wheels:

$$F_F = W \cdot \left(\frac{\mu l \cos \theta}{b - \mu h} \right) \quad (1)$$

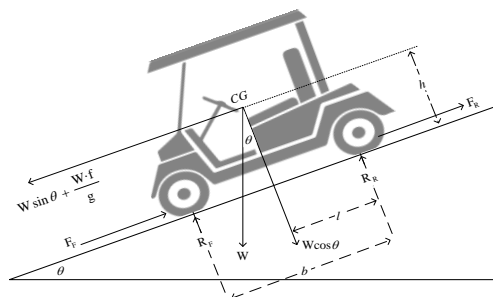


Fig. 1 Free body diagram of light-duty electric vehicle

Considering the braking force at the front wheels:

$$F_R = W \cdot \left(\frac{\cos \theta \cdot (b - l) \cdot \mu}{h \mu + b} \right) \quad (2)$$

Considering the braking force at the front wheels:

$$F_F + F_R = (\mu_F \cdot F_F) + (\mu_F \cdot F_R) \quad (3)$$

where R_F is the vertical reaction force between the road surface and the front wheels, R_R is the vertical reaction force between the road surface and the rear wheels, F_F is the braking force at the front wheels, W is the mass of the vehicle, $W \cdot f/g$ is the average force generated by wheel lockup, μ is the coefficient of friction between the vehicle's tires and the road, b is the wheelbase, h is the height distance between the road surface and the center of gravity (CG) point, l is the distance from the CG point to the center of the rear wheel.



3. Control System Design

Light electric vehicles, such as electric golf carts and bikes, are in the place of most people using vehicles rather than cars and heavy electric vehicles. Basic safety considerations are important [10]. The researchers can then focus on the hydraulic braking system. Since brake pressure control has a significant impact on braking efficiency, it has the advantage of increasing the precision and speed of the system control response, and it is easy to sense when the brake system is in trouble [11]. In design research related to safety systems, some factors must be considered, such as the system's efficiency and speed of response. The selection of the PD controller necessitates an understanding of the technical characteristics of the motor, as its parameters may vary over time [12].

In designing the PD controller used for golf cart control, it is employed to regulate the operation of a DC motor [13-15]. The notable advantage lies in the ability to adjust the control bandwidth of the DC motor. The selection of the PD controller necessitates an understanding of the technical characteristics of the motor, as its parameters may vary over time depending on the usage scenario. The control system's objective is to precisely control the hydraulic brake pressure following the input signal and align the DC motor with a second-order system dynamic. The control system diagram of the

pressure control system is shown in Fig. 2. A proportional-derivative (PD) control system with a transfer function $G_C(s)$ can be written as follows:

$$G_C(s) = K_p + K_d s \quad (4)$$

where K_p is a proportional component and K_d is a derivative component

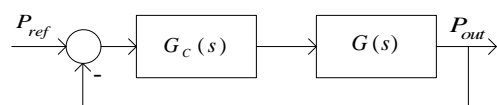


Fig. 2 Control system diagram of pressure control system

where P_{ref} is a pressure reference and P_{out} is a pressure output.

The design of the brake fluid pressure control system for light-duty electric vehicles has the position of the brake pedal control arranged, as shown in Fig. 3. The controller design can be divided into two parts: the design of the plant of the DC motor and the transfer function system.

3.1 Mathematical Model of the DC Motor

The mathematical model of the DC motor involves determining the parameters of the DC motor to facilitate the design of the control system. The gain value K is the sum of K_e and K_t [16], with the researcher knowing only the R of the DC motor. The parameters of the DC motor are shown in Table 1.

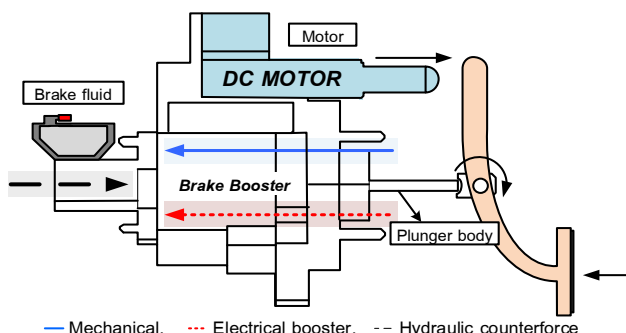


Fig. 3 Motor positioning for brake system oil pressure control

Table 1 Parameters of DC motor

Parameter	Value	Unit
R	10	Ω
Input voltage	24	Vdc
Load (Max)	500	N
Speed	13.5	mm/s
Stroke length	100	mm

This study focuses on exploring parameters for a DC motor intended to control the oil pressure in electric golf car brakes. The goal is to develop a safety system for users. Therefore, the analysis of the control system's performance is imperative to establish a mathematical model.

Fig. 4 displays the armature's electric equivalent circuit or DC motor model as well as the free-body schematic for the armature-controlled, separately excited DC motor [16].

MATLAB Simulink requires the development of a mathematical model to estimate parameters.

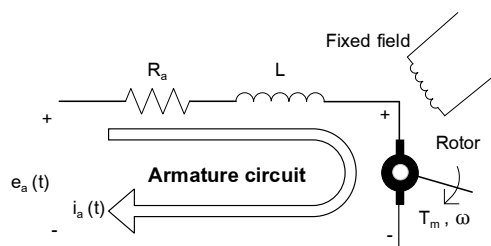


Fig. 4 DC motor model

The values of the variables will be simulated using the model. Through simulation in MATLAB Simulink, the researchers will enter the known electric resistance value into the model and determine the values of other parameters shown in Eq. (5):

$$G(s) = \frac{K}{(J \cdot L)s^3 + (J \cdot R + b \cdot L)s^2 + (K_e^2 \cdot b \cdot R)s} \quad (5)$$

where J is a moment of inertia of the rotor, b is a motor viscous friction constant, K_e is the electromotive force constant, and K_t is a motor torque constant, R is an electric resistance and L is an electric inductance.



System identification of the mathematical model is essential to investigate the relationship between input and output responses in the linear model's range. Given Eq. (5), the mathematical model of the system is Type 1. The PD controller is sufficient to control the system to meet the designed conditions with the knowledge of only one parameter, R , which is 10 ohms, the researchers need to estimate the values of other variables from the parameters in the equation. In the subsequent steps, these estimated values will be utilized in an optimization process to determine the PD controller using MATLAB Simulink program parameter estimation with Arduino uno R3 and MCT-HB-40A H-Bridge 10-30Vdc 40A. The parameters of the model are shown in Table 2.

Fig. 5 illustrates the pressure simulation responses of the system. It shows the pressure responses of the system with mathematical identification from the model compared to the experiment. By incrementally adjusting the hydraulic brake pressure in steps of 50 psi, starting from 50 psi to finishing at 200 psi, the method involved a systematic progression. This stepwise approach aimed to optimize and fine-tune the hydraulic brake pressure to achieve the desired performance or response in the system error 1.36%.

Table 2 Parameters of Mathematical Model

Parameter	Value	Unit
J	0.010178	$\text{kg} \cdot \text{m}^2$
K	0.40877	-
L	0.0039446	H
b	0.30469	$N \cdot \text{m} \cdot \text{s}$

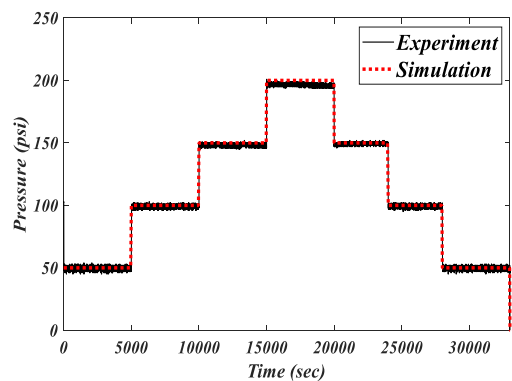


Fig. 5 Pressure simulation responses of the system

In designing the Mathematical Model for the DC Motor, the above-mentioned can be used to create a closed system control system diagram, as shown in Fig. 6.

3.2 Optimization of the PD Controller

The full dynamics, proportional control of the position error, and proportional control of the speed error are all included in the PD control with gravity compensation control algorithm [17]. P-Proportional and D-Derivative are the controllers that are the most widely used control algorithms, and the researcher chose P and D controllers for control of motor range [18], as shown in Fig. 7.

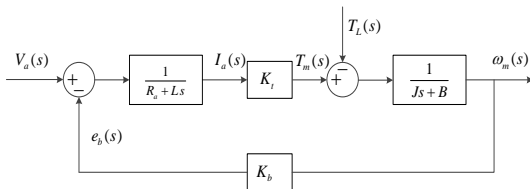


Fig. 6 Block diagram of the closed-loop speed control of the DC motor

where V_a is the armature voltage, i_a is the armature current, ω_m is the rotation speed (rad/s), e_b is the back electromotive force voltage (V), T_m is the motor torque (N.m), K_b is the back electromotive force coefficient (V.s/rad), B is the coefficient of viscous friction (N.m.s/rad,) and T_d is the external load disturbance (N.m).

The destination of the control system design is to create a system that responds to the common inputs in a desired way. It is preferable to have a transient reaction that oscillates just enough but not too much. A desirable steady-state response is one that precisely tracks the desired output [19,20] since the mathematical model of the equation system used in the research is shown in Eq. (5) in Section 3.1. Steady-state error for types of input system is of the $N = 1$ system type or Type-1; the selected control system was the PD Controller type.

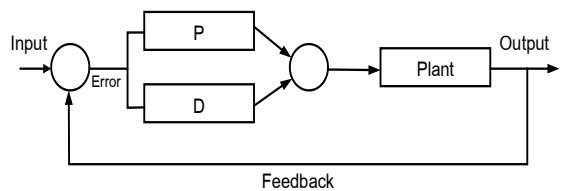


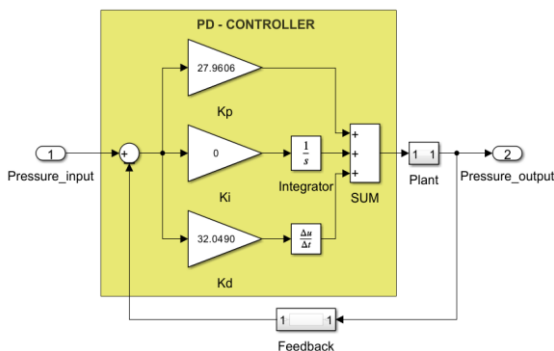
Fig. 7 The PD controller – non-interacting form schematic diagram

Since differentiating a noisy input leads to significant mistakes, the derivative term is not only undesirable but only roughly realizable. On the other hand, an analogous controller without differentiation is obtained if the output's derivative is monitored. Therefore, in practice, PD compensation is frequently possible. The specifications provided for the closed-loop system and the choice between a feedback controller determine how PD controllers are designed. Fig. 7 displays the system block diagram for a PD controller [19].

The parameters of the PD controller can be determined by using the signal constraints of the MATLAB Simulink program. Parameter and functional constraints limit the maximum overshoot by 10%, the rise time is 2 sec, the setting time is 4 sec, and the steady-state error is 5%. The result of this program is defined as shown in Table 3. The data in Table 3 was used in designing the optimized PD controller for controlling DC motors. This data can be used to create the control system diagram, as shown in Fig. 8.

**Table 3** Parameters of the PD controller

Parameter	Value
K_p	27.9606
K_d	32.0490

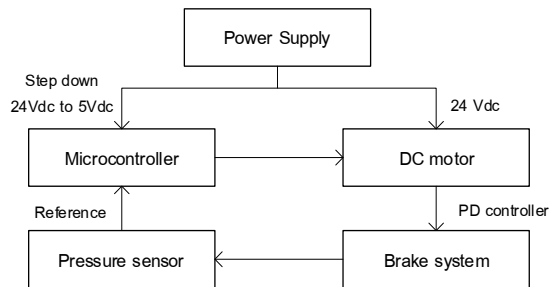
**Fig. 8** PD controller diagram of pressure control

4. Experiments

Regarding the brake oil pressure control testing, the researcher separated the experiment into two stages: experimental setup and experimental and simulation results. The latter displayed the system setup along with the experimental steps and compared the experimental results using actual equipment with the setup results. The experimental assessment employed statistical data and the root mean square error (RMSE) approach to evaluate the error findings.

4.1 Experimental setup

This section covers the experimental setup and the control system's dynamic responses. The experimental setup shown in Fig. 9 used a 24 Vdc supply from the power source, which was directed

**Fig. 9** Block diagram oil pressure control system

to both the DC motor and the microcontroller. A step-down converter was employed to reduce the voltage to 5 Vdc for operational purposes.

The DC motor was controlled by a PD controller to manage the braking system, and pressure readings from the brake fluid were obtained through a pressure sensor using WER 5 Vdc. The maximum pressure was 500 psi $\pm 2\%$ FS with a small output error. It had a complete surge voltage protection function.

4.2 Experimental and Simulation Results

The tests were divided into three experiments: constant, step, and harmonic pressure output. Constant pressure output is shown in Fig. 10. The comparison between simulation results and experimental data involved setting the constant value during the experiments at 100 psi. Additionally, the PD controller parameters were adjusted according to Table 3. The observed discrepancy with simulation between the simulated error and experimental error RMSE results was ± 1.85 psi.



Step pressure output is shown in Fig. 11. The simulation and experimental results comparison involved adjusting the step time from 0 s to 300 s, incrementing the final value by 50 psi at each step, and setting the sample time to 0.01 s. The observed discrepancy between the simulated and experimental error RMSE results is ± 2.56 psi.

Harmonic pressure output is shown in Fig. 12. The comparison between the simulation and experimental by adjusting the settings with a sine wave amplitude of 75, a bias of 125, and a frequency of 0.125 rad/sec, the graph exhibits a minimum point at a brake pressure of 50 psi and a maximum point at 200 psi. The observed discrepancy between the simulated and experimental error RMSE results is ± 7.89 psi.

The researchers used a PD controller, derived through optimization from the conducted trials, with K_p being 27.9606 and K_d being 32.0490, to regulate the hydraulic braking pressure for an electric golf cart. The brake pressure testing varied between 100 and 500 psi while maintaining a steady 20 km/h speed. That occurred to calculate the average stopping distance between the time the system went on and when the electric golf cart completely stopped.

Table 4 and Fig. 13 present the findings of the tests. From the results of the experiments of all three processes, namely constant, step, and harmonic, the responses with the maximum error values in order from the best to the worst were step > constant > harmonic

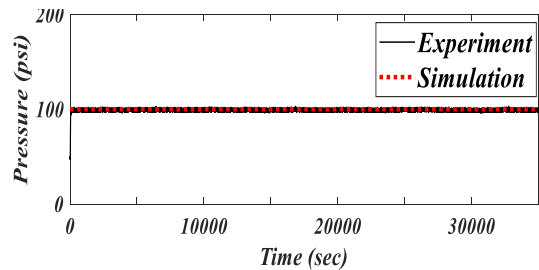


Fig.10 Constant pressure

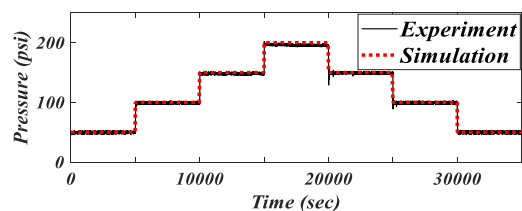


Fig. 11 Step pressure

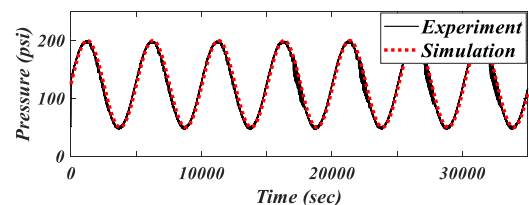


Fig. 12 Harmonic pressure

Table 4 Comparing the stopping distance of electric golf carts with the brake pressure used to control

Parameter (psi)	Distance (m)
100	31.43
200	18.23
300	12.25
400	6.76
500	6.57

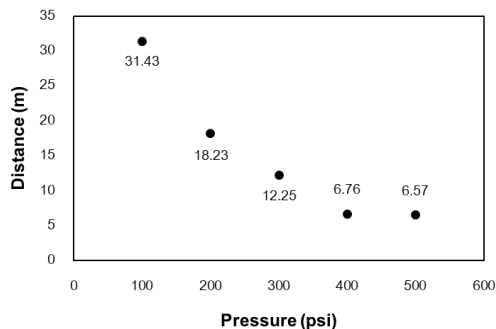


Fig. 13 Comparing the stopping distance

5. Conclusion

The research findings included a mathematical model for designing a PD controller for the braking system. The error value, when compared to the experiment, was 1.36%. This value was used to design a system controller capable of performing according to specified conditions. In the constant brake oil pressure experiment, there was an error of $\text{RMSE} \pm 1.85$ psi or a maximum error of 1.85%. The step brake oil pressure experiment had an error of $\text{RMSE} \pm 2.56$ psi or a maximum error of 1.28%, while the harmonic brake oil pressure experiment showed an error of $\text{RMSE} \pm 7.89$ psi or a maximum error of 3.95%. The experiment measured the braking distance of the vehicle at a constant speed of 20 km/h, utilizing brake fluid pressures ranging from 100 to 500 psi; the average stopping distances were 31.43, 18.23, 12.25, 6.76, and 6.57 m, respectively.

Regarding this experiment, there is a future trend towards developing an automatic braking assistance system. This study suggests potential advancements in brake control technology, aiming to enhance the overall efficiency of braking systems. Also, this design could be applied to larger vehicles.

In the future, the researcher expects that the experiment of controlling brake fluid pressure with a PD controller will be further developed in research by taking the system control process and PD parameter values obtained from this research to test in real vehicles by adding distance measurement sensors. It will measure the distance of obstacles in front while the objects are stationary by observing the relationship between the distance of the objects and the brake fluid pressure controlled by the control system and test the objects while they are moving in front of the vehicle to test the system response speed to see if the maximum efficiency is satisfactory.

6. Acknowledgement

This research was funded by College of Industrial King Mongkut's University of Technology North Bangkok. (Contract no. CIT-2022-GRAD-17)

7. References

- [1] <https://www.iea.org/reports/global-ev-outlook-2023>. (Accessed on 7 October 2024)

- [2] A.M. Maria, M. Biagi and R. Cusani, Vehicular technologies - deployment and applications: Smart vehicles, technologies and main applications in vehicular ad hoc networks, IntechOpen., Rijeka, Croatia, 2013.
- [3] K. Obeng, Injury severity, vehicle safety features, and intersection crashes, Traffic Injury Prevention, 2008, 9(3), 268–276.
- [4] T.J. Chengula, J. Mwakalonge, G. Comert and S. Siuhi, Improving road safety with ensemble learning: Detecting driver anomalies using vehicle inbuilt cameras, Machine Learning with Applications, 2023, 14, 100510.
- [5] M. Eskandari Torbaghan, M. Sasidharan, L. Reardon and L.C.W. Muchanga-Hvelplund, Understanding the potential of emerging digital technologies for improving road safety, Accident Analysis and Prevention, 2022, 166, 106543.
- [6] S. Han, H.W. Kim and J.H. Leigh, Improvement of road safety management systems of local governments in Korea after evaluating related indicators, Accident Analysis and Prevention, 2023, 193, 107325.
- [7] D.A. Lakhwani and D.M. Adhyaru, Performance comparison of PD, PI and LQR controller of autonomous under water vehicle, The Nirma University International Conference on Engineering (NUiCONE- India 2013), Proceeding, 2013, 1-6.
- [8] A. Deka and S.R. Basiredd, Emergency braking control in 3D overhead cranes using a switching PD-fuzzy controller, The International Conference on Control, Automation and Robotics (ICCAR-China 2023), Proceeding, 2023, 285-290.
- [9] X. He, H. Cheng, Z. Liu, J. Yang and T. Huang, Comparative study on anti-lock braking control strategies based on heavy-duty multi-axle special vehicles, The 2021 IEEE 4th Advanced Information Management, Communicates, Electronic and Automation Control Conference (IMCEC-China 2021), Proceeding, 2021, 780-785.
- [10] G. Subramaniam, K. Hari Adithyan, S. Gogul, D. Heera Sree and E. Kumaresan, Multi-model charger for light electric vehicles, The 2023 9th International Conference on Electrical Energy Systems (ICEES-India 2023), Proceeding, 2023, 418-421.
- [11] D. Pi, Q. Cheng, B. Xie, H. Wang and X. Wang, A novel pneumatic brake pressure control algorithm for regenerative braking system of electric commercial trucks, IEEE Access, 2019, 7, 83372-83383.
- [12] F. Golnaraghi and B. C. Kuo, Automatic control systems, 10th Ed., McGraw-Hill Education., NY, USA, 2017



- [13] X. Zhang, Design and implementation of fuzzy PID DC motor control system based on STM32, The 2023 IEEE International Conference on Control, Electronics and Computer Technology (ICCECT-China 2023), Proceeding, 2023, 1129-1131.
- [14] Y.B. Koca, Y. Aslan and B. Gokce, Speed control based PID configuration of a DC motor for an unmanned agricultural vehicle, The 2021 8th International Conference on Electrical and Electronics Engineering (ICEEE-Turkey 2021), Proceeding, 2021, 117-120.
- [15] S. Saengsri, S. Prawanta, S. Odngam and J. Srisertpol, PI-servo with state-D feedback and observer for magnetic stirrer machine, The 2017 International Conference on Circuits Devices and Systems (ICCDs-China 2017), Proceeding, 2017, 6–10.
- [16] B. Joshi, R. Shrestha and R. Chaudhary, Modeling simulation and implementation of brushed DC motor speed control using optical incremental encoder feedback, The Proceedings of IOE graduate conference (IOE-Nepal 2014), Proceeding, 2014, 497-505.
- [17] V. Prada-Jiménez, P.A. Niño-Suaréz, E.A. Portilla-Flores and M.F. Mauleodoux-Monroy, Tuning a PD+ controller by means of dynamic optimization in a mobile manipulator with coupled dynamics, IEEE Access, 2019, 7, 124712-124726.
- [18] M. Sreejeth, R. Kumar, N. Tripathi and P. Garg, Tuning a PID controller using metaheuristic algorithms, 2023 The 8th International Conference on Communication and Electronics Systems (ICCES-India 2023), Proceeding, 2023, 276-282.
- [19] M.S. Fadali and A. Visioli, Digital control engineering: Analysis and design, 3rd Ed., Elsevier Inc., Oxford, UK, 2009.
- [20] B. Chi-wu and X. Ke-fei, Robust control of mobile manipulator service robot using torque compensation, 2009 International Conference on Information Technology and Computer Science (ITCS-Ukraine 2009), Proceeding, 2009, 69-72.